Superdiffusive Motion of the Pb Wetting Layer on the Si(111) Surface

K. L. Man, M. C. Tringides, M. M. T. Loy, and M. S. Altman

Phys. Rev. Lett. **110**, 036104 — Published 18 January 2013

DOI: 10.1103/PhysRevLett.110.036104

Super-diffusive Motion of the Pb Wetting Layer on the Si(111) Surface

K.L. Man[1], M.C. Tringides[2], M.M.T. Loy[1] , M.S. Altman[1#]

[1]Department of Physics, Hong Kong University of Science and Technology, Kowloon, Hong Kong, China
[2]Ames Laboratory and Department of Physics, Iowa State University, Ames, IA 50011, U.S.A.

ABSTRACT

Mass transport in the Pb wetting layer on the Si(111) surface is investigated by observing non-equilibrium coverage profile evolution with low energy electron microscopy and micro-low energy electron diffraction. Equilibration of an initial coverage step profile occurs by the exchange of mass between oppositely directed steep coverage gradients that each move with unperturbed shape. The bifurcation of the initial profile, the shape of the profile between the two moving edges and the time dependence of equilibration are all at odds with expectations for classical diffusion behavior. These observations signal a very unusual coverage dependence of diffusion or may even reveal an exceptional collective super-diffusive mechanism.

E-mail: phaltman@ust.hk

PACS: 68.43.Jk, 68.35.Fx, 61.05.jh, 68.37.Nq

Atomic and molecular diffusion on solid surfaces [1] is critical to many physical and chemical phenomena, for example, epitaxial growth and the formation of surface-supported clusters and nanostructures [2-5], pattern formation [5,6], phase transformations [7], reactions and catalysis [6,8]. In each case, mass transport arises from collective diffusion, which is driven by the local concentration gradient. This driving force also causes the reduction of gradients in an initially non-uniform concentration profile to occur with sublinear time dependence, $\sim t^{1/2}$, characteristic of the underlying stochastic diffusion process, when it is allowed to evolve towards equilibrium. The stochastic nature of diffusion is similarly manifested in the random walk motion of a single isolated particle, whose root mean square displacement increases gradually with time as t^{γ}, with $\gamma = 1/2$ in the long time scale, diffusive regime. Alternatively, superdiffusion, with $\gamma > 1/2$, may also occur throughout nature on the long timescale, e.g. when particle motion involves rare but extreme long displacements, termed Lévy flights [9]. While superdiffusive motion may be expected to produce unique mass transport behavior, examples in epitaxial systems that demonstrate how this may occur and the implications for various physical and chemical processes are lacking.

A signature of exceptional mass transport in the Pb wetting layer on the Si(111) surface was originally evident in the formation of uniform height Pb island nanostructures on this surface, driven energetically by electron confinement [4,10]. Among systems that exhibit similarly induced structures, the self-organization in Pb/Si(111) stands out for its remarkable efficiency. Evidence of anomalous and exceptionally fast mass transport in Pb/Si(111) was also revealed through observations of non-equilibrium coverage profile evolution that were made using low energy electron

microscopy (LEEM) [11,12]. The linear temporal evolution by the motion of a non-dispersive coverage gradient at constant speed was seen in both an amorphous and the well ordered Pb/Si wetting layers. This contrasts with the profile broadening and sublinear temporal evolution that are observed in agreement with classical expectations during equilibration in other systems using the same or similar methods [13,14]. Diverse explanations that have been proposed to account for the non-classical behavior in Pb/Si(111) include the diffusion of thermally generated adatoms on top of the wetting layer [11] and coverage dependent diffusion, both phenomenological [12] and arising specifically in models of incommensurate overlayers under compressive strain [15,16].

In the present work, LEEM imaging [16,17] of profile evolution in Pb/Si(111) is complemented by precision micro-low energy electron diffraction (μLEED) measurements [18,19]. A rich sequence of "Devil's Staircase" (DS) and hexagonal incommensurate (HIC) structures forms in the coverage range 1.2 ML < θ < 1.33 ML that consists of different amounts and arrangements of ($\sqrt{7}$x$\sqrt{3}$) unit cells with θ = 1.2 ML and ($\sqrt{3}$x$\sqrt{3}$)R30° unit cells with θ = 1.33 ML [20,21]. This sequence offers the opportunity to determine coverage with an unprecedented combination of very high precision, on the order of ~0.001 ML, and high spatial resolution, ~ 2μm, and over macroscopic distances using μLEED. Surprising new results expose shortcomings of explanations that have been put forth to account for exceptional mass transport in Pb/Si(111) so far [11,12,15,16] and suggest intriguing alternative possibilities.

Non-equilibrium Pb coverage profiles were prepared by laser induced thermal desorption (LITD) [13,14]. A LEEM image series that depicts the establishment of a non-equilibrium profile in the Pb wetting layer by LITD and the ensuing profile evolution is

shown in Fig. 1 [22]. LITD produces a dark, roughly circular area in LEEM images of radius r_0 that is partially depleted of Pb and bounded by a sharp coverage step with steep gradient. Similar to earlier observations [11,12], the system equilibrates by the rapid motion of the coverage step profile radially inward from the perimeter of the LITD depleted area at constant speed and without broadening (Figs. 1(a)-(g)). The equilibration of Pb/Si(111) also exhibits a remarkable coverage dependence. The time required to refill the depleted area, τ, is independent of the initial wetting layer coverage (e.g. see Fig. 1(g)) when it exceeds a critical coverage, $\theta_i > \theta_c$, with $\theta_c = 1.241$ ML, while τ increases dramatically when θ_i is reduced below θ_c [11,12].

An even more dramatic effect unseen previously occurs outside the LITD depleted area (Fig. 1(b)-(f)). The edge of a modified region erupts outward from the perimeter of the LITD depleted area [22]. The initial speed of this expanding edge and the distance it travels decrease with increasing initial coverage prior to LITD (Fig. 1(g)). Its motion diminishes with time but still persists long after $t = \tau$. This extraordinary behavior was detected over a wide temperature range, from below 200K to at least 360K, provided $\theta_i > \theta_c$. The absence of the modification at lower coverage coincides with the divergence of τ.

We probed the nature of the modification to the wetting layer using μLEED. Fig. 2 shows μLEED patterns of various phases that form in Pb/Si(111) and metrics that characterize superstructure spot positions therein, which depend sensitively upon coverage [20,21]. The spot positions that are observed here when the Pb coverage is increased during continuous deposition at known rate (Fig. 2(i)) are consistent with previous reports [20,21]. We next exploit the sensitivity of diffraction spot positions to coverage to determine the Pb coverage profile very precisely.

The partially equilibrated configuration in Fig. 3(a) developed at 270K following LITD from a Pb film with DS phase structure at θ_i = 1.296 ML. Further evolution was arrested by rapidly cooling the sample below 150K prior to μLEED measurements. Fig. 3(a) also shows μLEED patterns of Pb phases that were obtained at the marked positions in the accompanying LEEM image. The Pb coverage profile is determined by comparing spot positions measured at different locations on the surface to spot positions that are calibrated against coverage independently (Fig. 2(i)). The Pb coverage profile that is determined along the line in Fig. 3(a) by this method is shown in Fig. 3(b). Interestingly, the coverage does not drop below θ_c and the profile has an exceptional concave shape, defined as having second derivative with respect to radial position that is positive, $\frac{\partial^2\theta}{\partial r^2} > 0$. There is also a surprisingly abrupt 0.04 ML coverage step at the expanding edge.

The modification of the wetting layer that occurs as the expanding edge passes is also revealed in dynamic coverage variations that are determined from time-dependent μLEED measurements at fixed position (Fig. 4). Following LITD at t = 0, the coverage remains unchanged until the coverage step at the expanding edge reaches the measurement position, at $t \approx 2$ sec in this example, identified as an abrupt drop of the coverage. Then, coverage drops more slowly to reach θ_c , at $t \sim \tau \approx 4$ sec, after which it recovers partially with sub-linear time dependence on a long time scale (>30τ). Pb that feeds this recovery is derived from the uninterrupted motion of the expanding edge at $t >$ τ (Fig. 1).

The non-dispersive motion of a coverage step profile has been observed in other systems [7,23,24]. The linear time dependence of the edge motion in those cases is a

result of a rate-limiting process of mass transfer across the moving edge. Models that have been considered so far to explain these spatial and temporal characteristics of profile evolution in Pb/Si(111) have also accounted for the lower cutoff θ_c for fast dynamics [11,12,15,16]. However, these models must now be viewed either as incorrect or incomplete in their present form because they fail to account for the bifurcation of the initial coverage step profile and the concave shape of the profile between the oppositely directed edges that are revealed experimentally here. Instead, these models uniformly predict convex profile shapes (defined as $\frac{\partial^2\theta}{\partial r^2} < 0$) in the source region and a smooth approach to θ_i at large distances.

By performing a Boltzmann-Matano (BM) type of analysis [7], we further explore the implications for previous models of Pb/Si(111) mass transport that either assume or exhibit coverage dependent diffusion mechanisms [12,14,15]. The oppositely directed motion of two steep coverage gradients implies two step-like changes of the coverage dependent diffusion coefficient, $D(\theta)$, that are likewise opposite. In particular, the moving edges at θ_c and $\theta_1 \geq 1.26$ ML indicate steep increase and decrease of $D(\theta)$ at these two coverages, respectively. The evolution of the concave profile shape between the two edges similarly relates to a decreasing $D(\theta)$. Quantitative analysis reveals a $D(\theta)$ that is sharply peaked at $\theta_c -$ with full-width-half-maximum of about 0.025 ML and rising to a maximum that is on the order of $3x10^3$ times greater than on either side of the peak – and that also drops steeply by another factor of order 10^2 at θ_1 [25]. In a Frenkel-Kontorova model of Pb/Si(111), the formation of soliton-like features that dominate mass transport over hopping of individual atoms gives rise to a single step-like increase of

$D(\theta)$ at θ_c [15]. However, a step-like increase of $D(\theta)$ of order 10^2 or more in current models can only account for the inward advancing profile edge motion in the desorption region [12,15]. Thus, these models cannot account fully for the experimental observations.

If the inexplicable coverage dependence of diffusion inferred from experimental observations is not the correct description of diffusion in this system, then the observed behavior has even more fundamental implications. The diffusion equation is straightforwardly constructed from the continuity equation, $d\theta/dt + \overline{\nabla} \cdot \bar{j} = 0$, and Fick's law expression for mass current density, $\bar{j}$. Local mass conservation, given irrefutably by the continuity equation, appears to be particularly problematic. According to Fick's law, which is postulated for stochastic diffusive processes, $\bar{j}$ is proportional to the gradient of the coverage, $\bar{j} = -D\overline{\nabla}\theta$. For the observed concave profile shape in the modified layer (Fig. 3(b)), the gradient, $\overline{\nabla}\theta$, hence the current density increases with increasing radial position (Fig. 3(c)). This implies that more mass arrives at a point in the modified layer than departs, consequently that Pb should accumulate and the coverage should increase (Fig. 3(c)). This contradicts the observation that the coverage only ever decreases in the modified wetting layer at $t < \tau$ (Fig. 3). This contradiction could therefore signal the failure of Fick's law and that diffusion is not driven by the local coverage gradient in the usual way.

Taken together, the non-classical and non-Fickian spatial and temporal profile evolution characteristics in Pb/Si(111) signal the presence of a distinctive, possibly non-stochastic mass transport mechanism. A collective super-diffusive mechanism, whereby the Pb layer slides cohesively over the substrate surface could explain the remarkable profile evolution behavior. Such motion may be related to the quasi-collective motion of

highly-mobile, hexagonally arranged strings of atoms embedded in the cubic Au(100) surface that was detected experimentally earlier [26]. This motion is believed to comprise numerous correlated single atom displacements that occur rapidly in sequence, if not instantaneously. The particular mechanism in Pb/Si(111) can be very efficient if it avoids inherently inefficient random walk diffusion processes. Such efficiency is essential for understanding the rapid motion of the refilling profile edge during profile evolution (up to 4 μm/sec at 270K in separate experiments), which is much higher than could be expected from Pb diffusion by thermally activated hopping [27,28].

Recent experiments in the kinetics of compressed Pb monolayers have shown unusual mobility and mass transport hinting to possible connections to the current experiments. For example, the decay of Pb islands on Ni(111) to equilibrium shapes is exceedingly fast and can only be accounted for by similar super-diffusive collective process as in Pb/Si(111). It was also found that a massive mesoscopic scale refacetting of the Si(557) surface occurs when the DS phase with $\theta > \theta_c$ is present at temperatures as low as 80K [30]. The high rate of mass transport needed for this refacetting to occur is analogous to the rapid mass transport observed here. In another study [31], the phase transition from a DS to a 2-d liquid phase in Pb/Si(111), slightly above room temperature, was studied with LEED and angle resolved photoemission spectroscopy to map out the electronic structure of the liquid phase. This experiment overlaps with the range of conditions used in the current study and can provide important information about possible links between the unusual mass transport and electronic effects. The direct Pb/Si(111) LEEM/μLEED experiments described in the current work and these experiments in the

recent literature should stimulate further work to identify the atomistic processes and origin of correlations that result in the super-diffusive motion of the Pb wetting layer.

Acknowledgments

Financial support from the Hong Kong Research Grants Council under Grant No. HKUST600109 is gratefully acknowledged. Work at the Ames Laboratory was supported by the Department of Energy-Basic Sciences under Contract DE-AC02_07CH11358.

References

1. R. Gomer, Rep. Prog. Phys. **53**, 917 (1990).
2. H. Brune, Surf. Sci. Rep. **31**, 121 (1998).
3. J.W. Evans, P.A. Thiel, M.C. Bartelt, Surf. Sci. Rep. **61**, 1 (2006).
4. K. Budde, E. Abram, V. Yeh, M.C. Tringides, Phys. Rev. B **61**, R10602 (2000).
5. R. Plass, J.A. Last, N.C. Bartelt, G.L. Kellogg, Nature **412**, 875 (2001).
6. G. Ertl, Science **254**, 1750 (1991).
7. A.T. Loburets, A.G. Naumovets, Y.S. Vedula, in *Surface Diffusion: Atomistic and Collective Processes* , ed M.C. Tringides (Plenum, New York, 1997), pp 509-528.
8. G. Ertl, in *Advances in Catalysis, Volume 45*, eds. B.C. Gates, H. Knözinger (San Diego, Academic Press, 2000), pp 1-69.
9. W.D. Luedtke and U. Landman, Phys. Rev. Lett. **82**, 3835 (1999).
10. T.C. Chiang, Surf. Sci. Rep. **39**, 181 (2000).
11. K.L. Man, M.C. Tringides, M.M.T. Loy, M.S. Altman, Phys. Rev. Lett. **101**, 226102 (2008).
12. M.C. Tringides, M. Hupalo, K.L. Man, M.M.T. Loy, M.S. Altman in *Nanophenomena at Surfaces: Fundamentals of Exotic Condensed Matter Properties*, ed. M. Michailov (Springer-Verlag, Berlin, Heidelberg, 2011), pp 39-64.
13. F. Heslot, A.M. Cazabat, P. Levinson, Phys. Rev. Lett. **62**, 1286 (1989).
14. C.M. Yim, K.L. Man, X. Xiao, M.S. Altman, Phys. Rev. B **78**, 155439 (2008).
15. L. Huang, C. Z. Wang, M. Z. Li, and K.M. Ho, Phys. Rev. Lett. **108**, 026101 (2012).
16. E. Granato and S. C. Ying, Tribology Lett. **48**, 83 (2012).
17. E. Bauer, Rep. Prog. Phys. **57**, 895 (1994).

18. M.S. Altman, J. Phys.: Condens. Matter **22**, 084017 (2010).

19. G.E. Thayer *et al*., Phys. Rev. Lett. **95**, 256106 (2005).

20. S. Stepanovsky, M. Yakes, V. Yeh, M. Hupalo, M.C. Tringides, Surf. Sci. **600**, 1417 (2006).

21. M. Yakes, V. Yeh, M. Hupalo, M.C. Tringides, Phys. Rev. B **69**, 224103 (2004).

22. See supplemental material at http://link.aps.org/supplemental/.....

23. J. Slezák et al., Phys. Rev. B **61**, 16121 (2000).

24. N. Ferralis *et al.,* Phys. Rev. Lett. **103**, 256102 (2009).

25. to be published.

26. M. Labayen, C. Ramirez, W. Schattke, O.M. Magnussen, Nature Matl. **2**, 783 (2003).

27. J.W.M. Frenken, B.J. Hinch, J.P. Toennies, Ch. Wöll, Phys. Rev. B **41**, 938 (1990).

28. L. Kuipers and J.W.M. Frenken, Phys. Rev. Lett. **70**, 3907 (1993).

29. T.R.J. Bollmann, R. van Gastel, H.J.W. Zandvliet, B. Poelsema, Phys. Rev. Lett. **107**, 136103 (2011).

30. M. Czubanowski, A. Schuster, H. Pfnür, C. Tegenkamp, Phys. Rev. B **77**, 174108 (2008).

31. K.S. Kim and H.W. Yeom, Phys. Rev. Lett. **107**, 136402 (2011).

Figure Captions

Figure 1: LEEM image sequence [22] of profile evolution in Pb/Si(111) at times (a) < 0, (b) 0.2 s, (c) 4 s, (d) τ = 8 s, (e) 16 s, (f) 32 s following LITD (T = 270K, θ_i = 1.297 ML, LITD radius r_0 = 16 μm). (g) The radial positions of the refilling edge inside the LITD area and the expanding edge are plotted versus time for different initial coverages, θ_i (T = 270 K, r_0 = 26 μm).

Figure 2: μLEED patterns of (a) (√7x√3) at θ = 1.193 ML, (b) DS (*n*,*1*) at 1.219 ML (c) HIC at 1.245 ML and (d) DS (*1*,*m*) at 1.297 ML phases (m,n = integer) centered at the (√3x√3) (1/3, 1/3) positions. The schematic (e) (√7x√3), (f) DS (*n*,*1*), (g) HIC, and (h) DS (*1*,*m*) diffraction patterns identify the metrics H, H', δ and ϕ that quantify the satellite spot positions. Dimensions as per centages of the Brillouin zone (BZ) are indicated. (i) Variation of δ (○) and H' (□) as a function of Pb coverage during Pb deposition at T = 263K.

Figure 3: (a) μLEED patterns obtained in the (1) unfilled LITD area (θ = 1/3 ML), (2) refilled LITD area, (3)-(5) modified wetting layer, (6) unmodified Pb wetting layer at the positions indicated in the accompanying LEEM image. The coverage profile in (b) is determined from the diffraction spot positions at locations along the line in (a). (c) The mass current densities arriving (solid arrow) and departing a point (dashed arrow) imply local mass accumulation, $\left[\partial\theta/\partial t\right]_{CE} > 0$, for concave profile shape according to the continuity equation (CE). Mass depletion is observed experimentally, $\left[\partial\theta/\partial t\right]_{obs} < 0$.

Figure 4: The Pb coverage determined locally by μLEED at a position 100 μm from the perimeter of the LITD area (r_0 = 30 μm) is plotted versus time following LITD at t = 0 on short (left) and long time scale (T = 300K, θ_i = 1.287 ML).

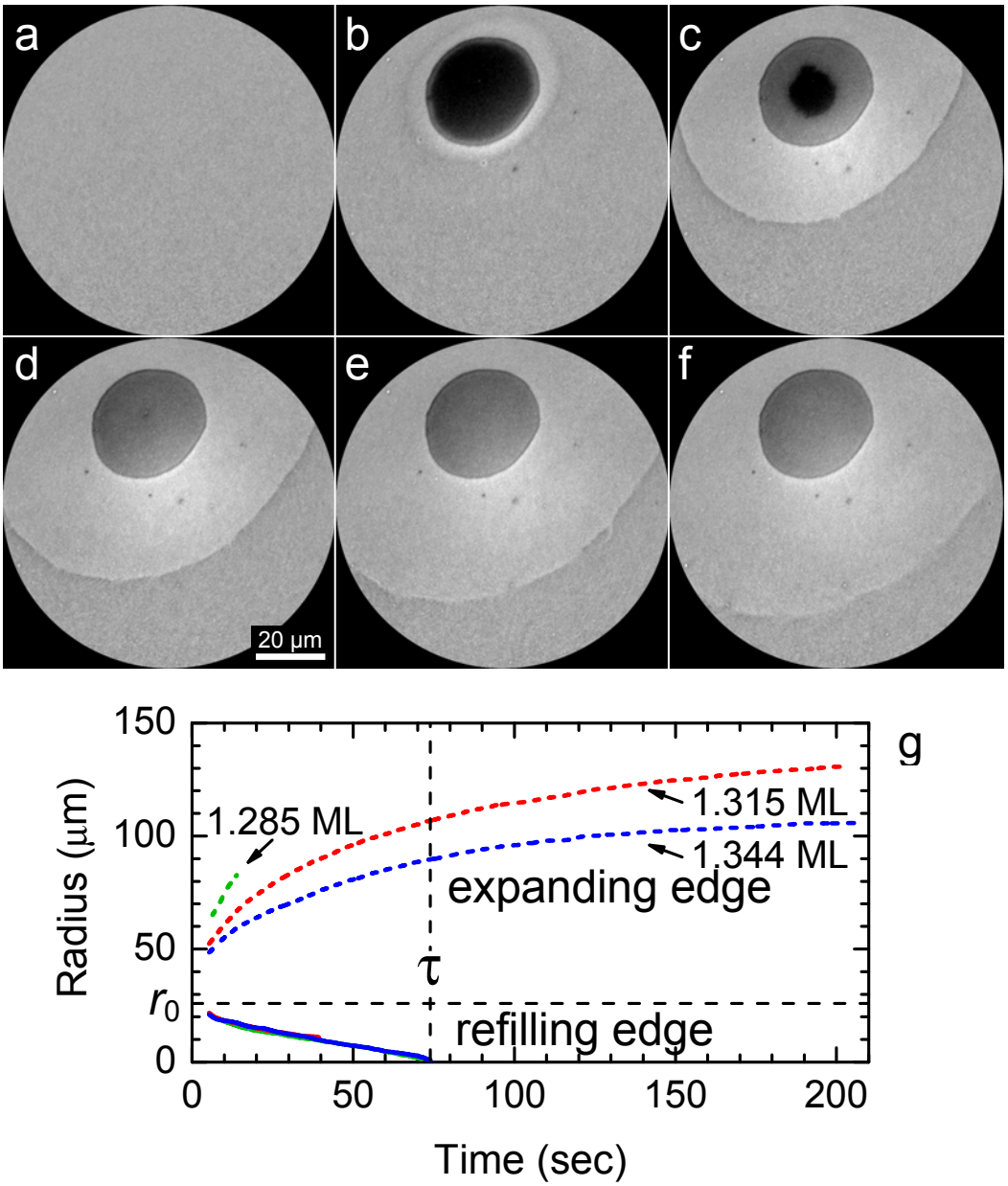

Fig. 1 (K.L. Man *et al*.)

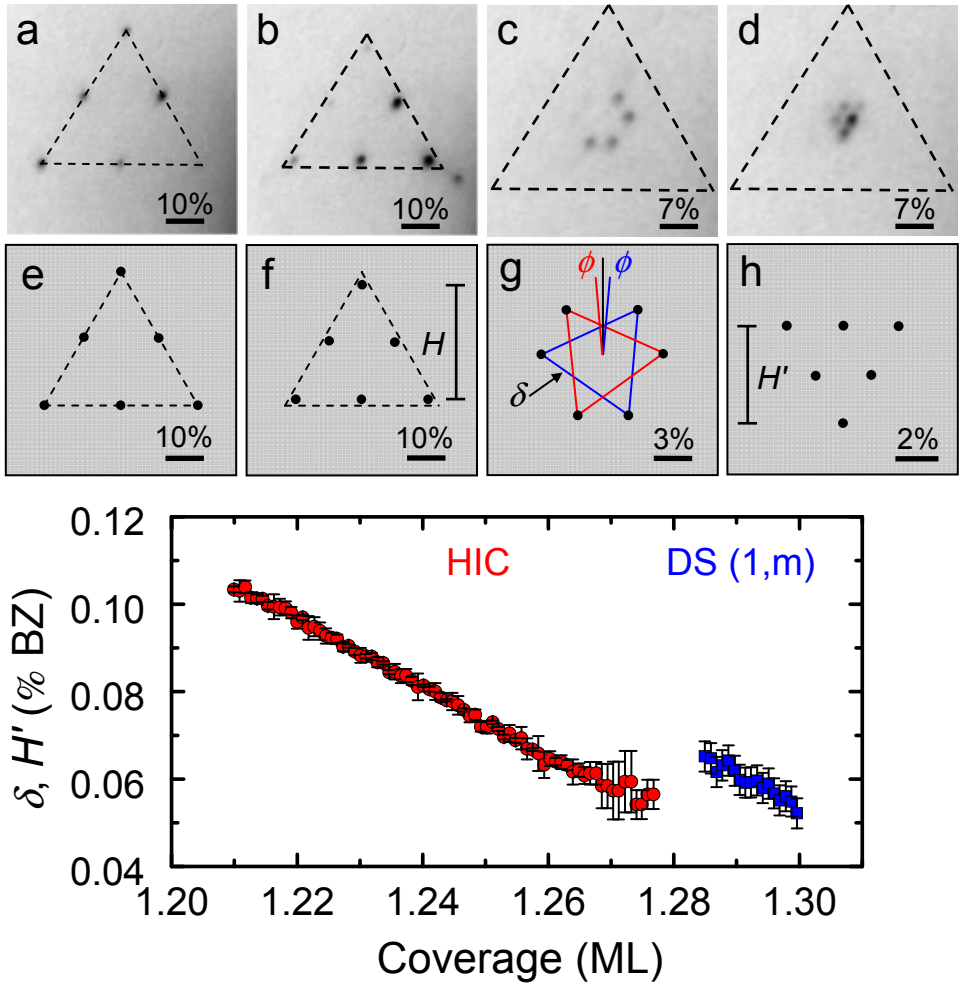

Fig. 2 (K.L. Man *et al*.)

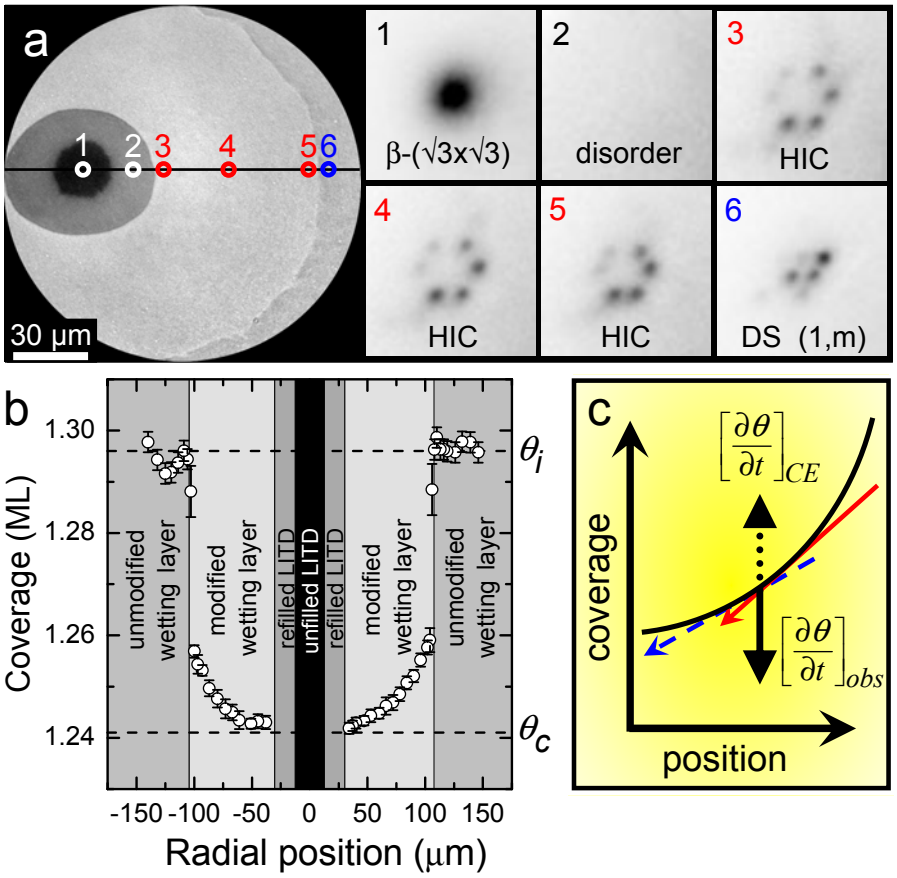

Fig. 3 (K.L. Man *et al*.)

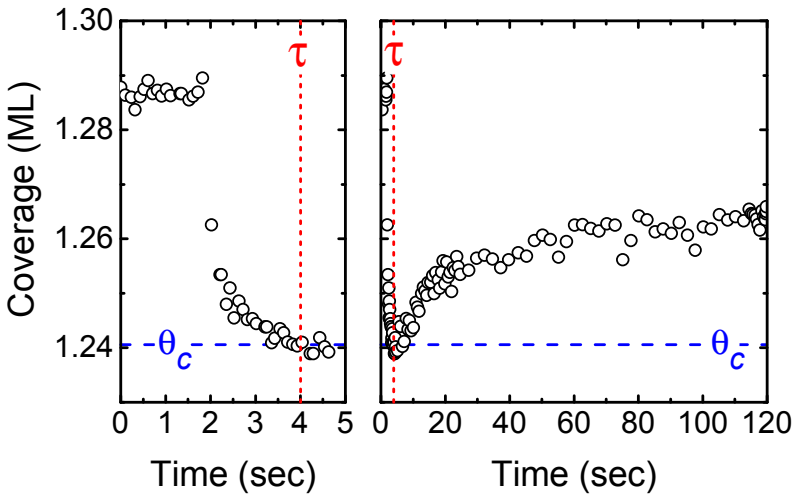

Fig. 4 (K.L. Man *et al*.)